

## N-face high electron mobility transistors with a GaN-spacer

M. H. Wong<sup>\*,1</sup>, S. Rajan<sup>1</sup>, R. M. Chu<sup>1</sup>, T. Palacios<sup>\*\*1</sup>, C. S. Suh<sup>1</sup>, L. S. McCarthy<sup>1</sup>,  
S. Keller<sup>1</sup>, J. S. Speck<sup>2</sup>, and U. K. Mishra<sup>1</sup>

<sup>1</sup> Electrical and Computer Engineering Department, University of California, Santa Barbara,  
CA 93106-9560, USA

<sup>2</sup> Materials Department, University of California, Santa Barbara, CA 93106-5050, USA

Received 30 September 2006, revised 25 December 2006, accepted 5 January 2007

Published online 16 May 2007

PACS 73.40.Kp, 73.61.Ey, 81.05.Ea, 85.30.De, 85.30.Tv

N-face AlGaIn (cap)/GaN (channel)/AlGaIn (barrier)/GaN (buffer) high electron mobility transistors (HEMTs) provide a simple solution for strong confinement of the two-dimensional electron gas (2DEG) from the back since carriers are induced on top of the AlGaIn barrier. To reduce the adverse effects of random alloy scattering from the AlGaIn barrier, an N-face GaN-spacer HEMT was designed with an epitaxial structure consisting of an AlGaIn (cap)/GaN (channel)/AlN/GaN (spacer)/AlGaIn (barrier)/GaN (buffer). The 2DEG is confined at the GaN (channel)/AlN interface, while the GaN-spacer layer separates the 2DEG from the AlGaIn barrier. The large polarization-induced electric field of the AlN and its large conduction band discontinuity with GaN provide strong confinement for good pinch-off and low output conductance under high electric fields. Up to 20% improvement in electron mobility was measured in these devices. The devices showed a current gain cut-off frequency ( $f_t$ ) of 24 GHz and power gain cut-off frequency ( $f_{max}$ ) of 44 GHz for a nominal gate length of 0.7  $\mu\text{m}$ . An output power density of 4.5 W/mm was measured at 4 GHz, with 34% power added efficiency and a gain of 10.3 dB at a drain bias of 40 V.

© 2007 WILEY-VCH Verlag GmbH & Co. KGaA, Weinheim

### 1 Introduction

Recent advances in materials growth and device technology have made gallium nitride an excellent candidate for high power microwave applications [1–4]. Most device research has been carried out on Ga-face (0001) materials. N-face (000 $\bar{1}$ ) materials, with their reversed direction of polarization, open up possibilities for many new device designs. The two-dimensional electron gas (2DEG) in a conventional N-face (000 $\bar{1}$ ) HEMT is induced on top of the AlGaIn barrier (Fig. 1), which is opposite to the case of Ga-face AlGaIn/GaN HEMTs. Therefore, the AlGaIn layer itself provides a strong back barrier for confinement of the 2DEG – this natural back barrier can reduce short channel effects [5–8]. The need for additional engineering design to enhance electron confinement in Ga-face HEMTs (e.g. an InGaIn back barrier [9]) is eliminated with the use of N-face materials. However, strong random alloy scattering from the AlGaIn can degrade the transport properties of the 2DEG. In this work, we present an N-face HEMT where the 2DEG is confined at a GaN/AlN hetero-interface, separated from the AlGaIn barrier by a GaN-spacer layer (Fig. 2). This design mitigates the adverse effects of the AlGaIn barrier on 2DEG transport properties in N-face HEMTs, as will be explained in the following section.

\* Corresponding author: e-mail: mh Wong@ece.ucsb.edu, Phone: +1 (805) 893 3812 (x204), Fax: +1 (805) 893 8714

\*\* Currently with the Department of Electrical Engineering and Computer Science, Massachusetts Institute of Technology, Cambridge, MA

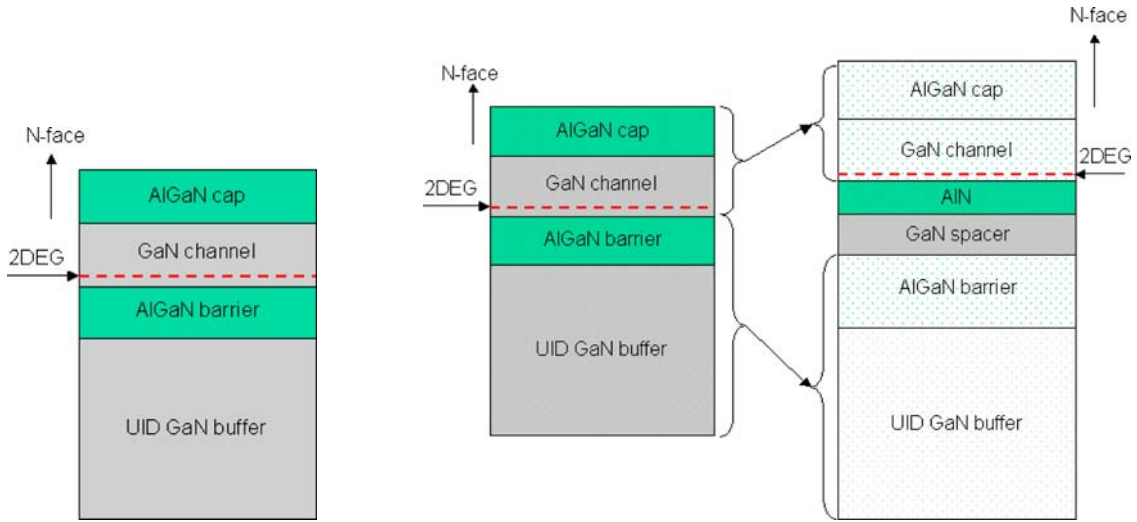


**Fig. 1** (online colour at: www.pss-a.com) Layer structure of a conventional N-face HEMT.

**Fig. 2** (online colour at: www.pss-a.com) N-face HEMT with GaN-spacer layer and AlN for 2DEG confinement.

## 2 Device design and fabrication

All devices in this work were grown in a Varian Gen-II plasma-assisted nitride MBE machine at 720 °C. The device structure is depicted in Fig. 3. The substrates were C-face 6H-SiC which received chemical-mechanical polishing from NovaSiC. A two-step ~0.5 μm thick GaN buffer was used to reduce threading

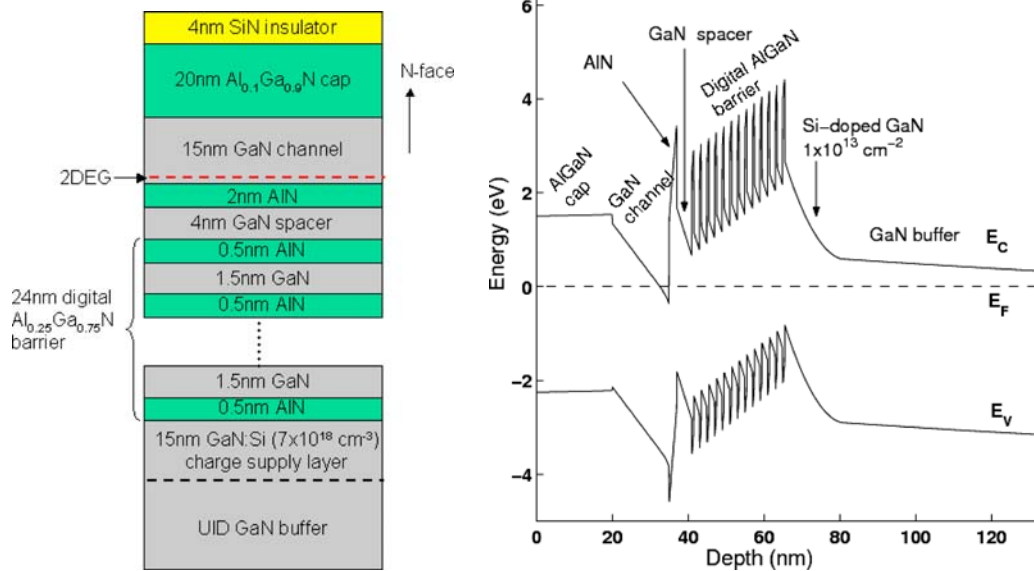


**Fig. 3** (online colour at: www.pss-a.com) Layer structure and simulated band diagram (generated by 1D Schrödinger–Poisson solver [10]) of the N-face GaN-spacer HEMT.

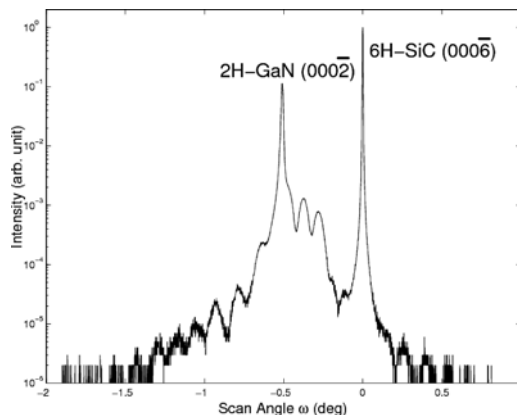


Fig. 4  $\omega$ - $2\theta$  X-ray scan of the N-face GaN-spacer HEMT.

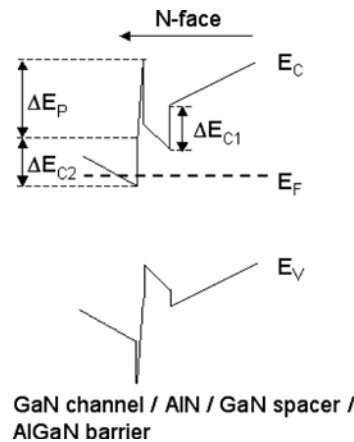


Fig. 5 Schematic band diagram of N-face GaN-spacer HEMT.

dislocation density to the low  $10^{10} \text{ cm}^{-2}$  [5]. A 24 nm  $\text{Al}_{0.25}\text{Ga}_{0.75}\text{N}$  barrier layer was grown on top of a Si-doped region ( $1 \times 10^{13} \text{ cm}^{-2}$ ) to help induce charges in the channel, followed by a 4 nm GaN-spacer, 2 nm AlN and 15 nm GaN channel layer. The devices were capped by 20 nm  $\text{Al}_{0.1}\text{Ga}_{0.9}\text{N}$  to increase the breakdown voltage [7, 8]. Since the MBE system was only equipped with one Al cell, the  $\text{Al}_{0.25}\text{Ga}_{0.75}\text{N}$  layer was grown digitally as a twelve-period AlN/GaN (0.5 nm/1.5 nm) superlattice instead of a ternary alloy (i.e. supplying Al, Ga and N fluxes simultaneously) to avoid growth interruption at the AlN, after which the Al flux was dropped for the  $\text{Al}_{0.1}\text{Ga}_{0.9}\text{N}$  cap grown as a ternary alloy. High resolution X-ray scan of the resultant heterostructure exhibited clear diffraction fringes, indicating good structural quality without intermixing in the superlattice (Fig. 4). A 4 nm  $\text{SiN}_x$  insulator was deposited by MOCVD prior to device processing to suppress gate leakage.

Devices were fabricated with Ti/Al/Ni/Au (20/100/10/50 nm) ohmic metallization, annealed at 870 °C for 30 s in  $\text{N}_2$  atmosphere. Mesa isolation was done with chlorine-based reactive ion etch. Ni/Au/Ni (30/250/50 nm) metallization was used for the gates. The surface was subsequently passivated with  $\text{SiN}_x$  deposited by PECVD. All devices were  $2 \times 75 \mu\text{m}$  wide with 0.7  $\mu\text{m}$  nominal gate length and 0.7  $\mu\text{m}$  gate-source spacing. The ohmic source-drain spacing was 3.4  $\mu\text{m}$ .

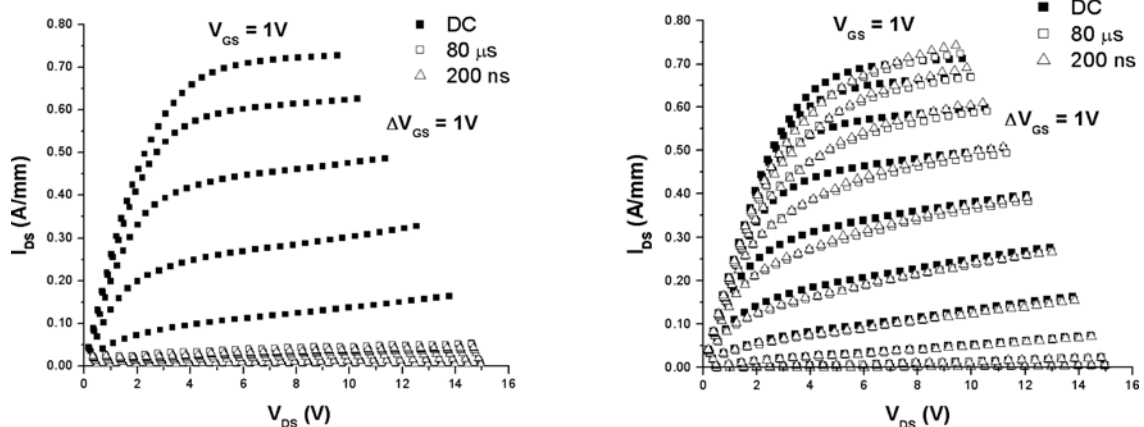


Fig. 6 DC and pulsed-IV (80  $\mu\text{s}$  and 200 ns pulse-widths) measurements on 50  $\Omega$  load line. Left: Before passivation; Right: After  $\text{SiN}_x$  passivation.

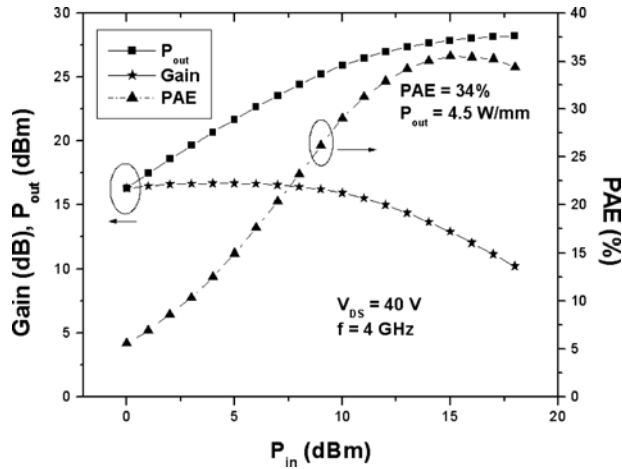


Fig. 7 Load-pull power measurement at 4 GHz of an N-face GaN-spacer HEMT.

A schematic band diagram of the N-face GaN-spacer HEMT is shown in Fig. 5. The larger conduction band discontinuity of GaN with AlN than with AlGaIn ( $\Delta E_{c2} > \Delta E_{c1}$ ) as well as the large dipole ( $\Delta E_p$ ) of AlN strained to GaN enable the use of a thin layer (2 nm) of AlN for stronger back barrier confinement than with an AlGaIn alloy [11]. Electrons confined at the GaN/AlN interface do not experience scattering from a ternary random alloy and thus exhibit higher mobility. Under high field conditions, energetic electrons whose wavefunctions penetrate the AlN experience the same effective mass in the GaN-spacer instead of a higher effective mass in the AlGaIn. Higher effective electron velocity is therefore expected with a GaN-spacer design, which has been demonstrated in Ga-face HEMTs [12].

### 3 DC and RF characterization

Room temperature Hall measurements with the Van der Pauw geometry revealed a 2DEG density of  $7 \times 10^{12} \text{ cm}^{-2}$  with mobilities ranging from 1550 to 1750  $\text{cm}^2/\text{Vs}$ , which were 20% higher than in conventional N-face HEMTs [7]. A maximum drain current  $I_{\text{max}}$  of 0.73 A/mm and an extrinsic transconductance of 133 mS/mm were achieved. Improved values are expected after optimizing the ohmic contacts, which were in excess of  $1 \Omega \text{ mm}$  in these devices. Two terminal gate-drain breakdown at 1 mA/mm was in excess of 55 V. Current–voltage measurements under DC and 200 ns pulsed conditions with the device biased on a  $50 \Omega$  load line indicated a limited amount of DC-RF dispersion (Fig. 6).

Small signal s-parameter measurements were performed with an Agilent E8361A network analyzer. The  $f_t$  and  $f_{\text{max}}$  were found by linear extrapolation of the current gain and power gain respectively along a 20 dB/dec slope. A maximum  $f_t$  of 24 GHz and  $f_{\text{max}}$  of 44 GHz were achieved at  $I_{\text{DS}} = 267 \text{ mA/mm}$  and  $V_{\text{DS}} = 15 \text{ V}$ . Power measurements were performed using a Maury microwave load-pull system. Measurements at 4 GHz with a drain bias of 40 V and quiescent current of 293 mA/mm yielded a transducer gain  $G_T$  of 10.3 dB at the maximum output power density  $P_{\text{out}}$  of 4.5 W/mm with power added efficiency (PAE) of 34% (Fig. 7). These are the first microwave power measurements on N-face transistors. Some large-signal dispersion was still observed under RF excitation, and we expect improved output power density and efficiency after optimization of the  $\text{SiN}_x$  passivation technology for N-face surfaces.

### 4 Conclusion

N-face HEMTs using a GaN-spacer and AlN layer for extra electron confinement have been realized. Lower alloy scattering has led to significant improvements in mobility. With improved growth and processing technologies for reducing gate leakage and preventing dispersion, microwave power capability in N-face transistors was demonstrated. The design strategy and results of this work promise high-performance mm-wave HEMTs based on N-face materials.

**Acknowledgements** The authors gratefully acknowledge funding from the AFOSR (G. Witt and K. Reinhardt), CNID and the ONR MINE MURI project (H. Dietrich and P. Maki).

## References

- [1] Y.-F. Wu, A. Saxler, M. Moore, R. P. Smith, S. Sheppard, P. M. Chavarkar, T. Wisleder, U. K. Mishra, and P. Parikh, *IEEE Electron Device Lett.* **25**, 117 (2004).
- [2] A. Chini, D. Buttari, R. Coffie, L. Shen, S. Heikman, A. Chakraborty, S. Keller, and U. K. Mishra, *IEEE Electron Device Lett.* **25**, 229 (2004).
- [3] S. Rajan, P. Waltereit, C. Poblenz, S. J. Heikman, D. S. Green, J. S. Speck, and U. K. Mishra, *IEEE Electron Device Lett.* **25**, 247 (2004).
- [4] J. S. Moon, M. Micovic, P. Janke, P. Hashimoto, W.-S. Wong, R. D. Widman, L. McCray, A. Kurdoghlian, and C. Nguyen, *Electron. Lett.* **37**, 528 (2001).
- [5] S. Rajan, M. Wong, Y. Fu, F. Wu, J. S. Speck, and U. K. Mishra, *Jpn. J. Appl. Phys.* **44**, L1178 (2005).
- [6] S. Rajan, A. Chini, M. Wong, C. Suh, Y. Fu, M. J. Grundmann, F. Wu, J. S. Speck, and U. K. Mishra, 32nd International Symposium on Compound Semiconductors (ISCS), Europa-Park Rust, Germany, 18–22 Sept. 2005.
- [7] S. Rajan, A. Chini, M. H. Wong, J. S. Speck, and U. K. Mishra, submitted to *J. Appl. Phys.*, Dec. 2006.
- [8] S. Rajan, Ph.D. Thesis, University of California at Santa Barbara (2006).
- [9] T. Palacios, A. Chakraborty, S. Heikman, S. Keller, S. P. DenBaars, and U. K. Mishra, *IEEE Electron Device Lett.* **27**, 13 (2006).
- [10] M. Grundmann, *BandEng*, Available online: <http://www.michaelgrundmann.com>.
- [11] S. Keller, S. Heikman, L. Shen, I. P. Smorchkova, S. P. DenBaars, and U. K. Mishra, *Appl. Phys. Lett.* **80**, 4387 (2002).
- [12] T. Palacios, L. Shen, S. Keller, A. Chakraborty, S. Heikman, S. P. DenBaars, U. K. Mishra, J. Liberis, O. Kiprijanovic, and A. Matulionis, *Appl. Phys. Lett.* **89**, 073508 (2006).